Acoustic Detection of Greenhouse-induced Climate Changes in the Presence of Slow Fluctuations of the Thermohaline Circulation

UWE MIKOLAJEWICZ AND ERNST MAIER-REIMER

Max-Planck-Institut für Meteorologie, Hamburg, Germany

TIM P. BARNETT

Scripps Institution of Oceanography, La Jolla, California

(Manuscript received 1 August 1991, in final form 16 April 1992)

ABSTRACT

Munk and Forbes have proposed to detect greenhouse gas–induced climate changes in the World Ocean with an array of long-range acoustic transmissions from Heard Island in the southern Indian Ocean. We estimated—assuming a continuously monitorable simplified axial ray propagation—the signal-to-noise ratio for such an experiment in an environment of slow fluctuations of the thermohaline circulation on a decadal time scale. The signal and noise are obtained from two coarse-resolution ocean general circulation model simulations. In the first, prescribed greenhouse atmospheric anomalies forced the ocean and yielded rough estimates of ocean response to greenhouse warming. In the second, some aspects of low-frequency internal variability of the ocean were obtained by stochastic forcing of the same ocean model. By this technique, no oscillations of the coupled ocean–atmosphere system like, for instance, El Niño–Southern Oscillation (ENSO) could be stimulated. Both signal and internal variability proved to be strongest at high latitudes, where the depth of the sound channel is small. At lower latitudes the signal is relatively weak, except for the western Atlantic. An array with an acoustic source near Heard Island would monitor primarily temperature changes in the near-surface layers of the Southern Ocean rather than in low-latitude intermediate depths.

The trend detection probability for any single path came out to be weak, at least for a one-decade measuring interval. But using information from at least a two-decade interval and an array of receivers improved the detection probabilities substantially. Two different pattern detection strategies were tested: projecting the natural variability on the expected greenhouse signal and projecting the greenhouse signal onto the major components of the natural variability. Both techniques proved to give almost identical results.

1. Introduction

The problem of detecting climate changes expected as a consequence of the increase of atmospheric greenhouse gases (GHG) has become increasingly important. Several attempts have been made to analyze historical data records and to compare them with the expected signal in both surface ocean and air temperature (e.g., Barnett 1986; Barnett and Schlesinger 1987; Santer et al. 1991; Barnett 1991) and ocean hydrographic data (e.g., Barnett 1983). Munk and Forbes (1989, henceforth MF) have proposed measuring the changes in travel times of long-distance acoustic transmissions from Heard Island in the southern Indian Ocean to receivers scattered around other ocean basins. One would use the change in the travel times (presumably decreasing with increased GHG concentrations) over a period of years as a detection strategy since they are primarily a measure of the average temperature change along the acoustic ray paths (the sound speed depends also, to a lesser degree, on salinity). This "acoustic thermometer" (as proposed by Spiesberger et al. 1983) has the advantage of producing integrated quantities, thus significantly reducing the noise level from measurements at individual locations and hence minimizing the higher-frequency noise problems mentioned by earlier authors. Spiesberger and Metzger (1991) have demonstrated the practical feasibility of this method at least on a basin scale (3000 km). For the experiments described in this paper, we took it as given that the method would be feasible on the semiglobal scale, too, but we realize that up to now there has been no generally accepted evidence for justification of this assumption.

The eddy-induced changes of sound speed in the high-frequency range of the natural variability were investigated by Semtner and Chervin (1990) using a simulation with a global eddy-resolving ocean general circulation model (OGCM). They concluded that the presence of eddies would not be a serious difficulty for the detection strategy of MF. The contribution from individual eddies is averaged out through the integra-

Corresponding author address: Uwe Mikolajewicz, Max-Planck-Institut für Meteorologie, Bundesstr. 55, D-2000 Hamburg 13, Germany.

tion over long paths. However, one still has to deal with the problem of decadal and longer time-scale natural variability and its effect on the acoustic transmission. For instance, would it be possible to discriminate the temperature rise at the end of the Little Ice Age (fifteenth to eighteenth century) from the expected greenhouse gas signal? How different is the structure of the expected warming from those of natural variability? If the expected signal is measured, how sure can we be that it is really a direct result of the greenhouse effect and not due to natural variability?

Proper detection studies will require knowledge of both the greenhouse signal and the natural variability. Unfortunately, very little is known about variability on decadal and longer time scales. It is very difficult, if not impossible, to derive estimates from historical observations alone. The only alternative is to obtain the required information from climate models. Whereas it is now possible to derive estimates of the greenhouse signal from simulations with coupled atmosphere and ocean general circulation models, the length of the simulations required for a reliable estimate of the naturally occurring long-term variability is of the order of 1000 years. Only such simulations make it possible to discriminate between natural variability of the system and model drift. Due to the high computational costs of coupled atmosphere and ocean models, published simulations have not exceeded 100 years (Stouffer et al. 1989; Cubasch et al. 1991; Manabe et al. 1991). The most computationally intensive part of these coupled models is the atmospheric component. The very rapid changes in the atmosphere put an upper limit on the achievable model time step. On the time scales of decades and longer, the atmosphere is more or less in statistical equilibrium with ocean and ice sheets. On these time scales, an appropriate simplification of the coupled system is to represent the atmosphere by a prescribed climate with white noise added and to investigate the response of an OGCM to that forcing. This is essentially the concept of the stochastic climate models as introduced by Hasselmann (1976). The resulting reddening of the oceanic response is due to two effects: one is simply the integration of atmospheric disturbances and the other is the stimulation of possible natural modes of the oceanic variability. The first effect has been exploited in several simple stochastic climate models with linear feedback terms (e.g., Lemke 1977; Reynolds 1979; Wigley and Raper 1990). The combination of both effects has been investigated in a more complex stochastic climate model by Mikolajewicz and Maier-Reimer (1990, henceforth MM), who forced an OGCM with climatological atmospheric boundary values plus white noise freshwater fluxes.

In this paper we use the variability occurring in the MM experiment as an estimate of the low-frequency part of the natural variability spectrum, and we attempt an estimate of the signal-to-noise (S/N) ratio typical for the experiment proposed by MF. Due to the strong simplifications underlying our approach, all probabilities given below do not include estimates of the model uncertainties, and are estimates of the order of magnitude rather than of the exact probability of greenhouse effect detectability. We focus on methodologies for handling the S/N problem in oscillations on decadal time scales, for which the results of a relatively short oscillation interval would be indistinguishable in observations from a real trend. We clearly emphasize that our method disregards completely any kind of shorter time-scale variations such as ENSO, eddies, or even microturbulence, which should be monitored simultaneously during the experiment. Due to the coarse vertical resolution of our model, the position of the sound speed minimum remains constant at the depth of 1 km in most parts of the ocean; consequently, we cannot address effects of small changes in the depth of the sound track on the travel time. Nevertheless, the results give a first indication of the principal reliability of the MF detection strategy assuming, of course, that the monitoring experiment is technically feasible. Heard Island itself will probably not serve as persistent carrier of a transmitter station, due to logistical problems in that remote area. We suggest, however, that our methodology will be easily transferred to any other planned network of transmitter–receiver stations. In any case, more experiments are required to confirm the present results. This will be the subject of future work.

2. The ocean model

The large-scale geostrophic OGCM, as conceptually proposed by Hasselmann (1982), is especially designed for the study of long period climatic fluctuations. Some basic features of this model have been described in Maier-Reimer et al. (1993). An implicit integration method permits a time step of 30 days, thus allowing integrations over thousands of years at acceptable computing cost.

The model is based on the conservation laws of salt, heat, and momentum. The advection of momentum is neglected, and the hydrostatic assumption together with the Boussinesq approximation have been applied. The continuity equation and the assumption of incompressibility of the fluid allow the derivation of the vertical velocities from the divergence of the horizontal components. The density is given by the full equation of state. A simple one-layer sea ice model with viscous rheology is included. The present application of this model has a horizontal resolution of $3.5° \times 3.5°$ and 11 vertical levels (centered at depths of 25, 75, 150, 250, 450, 700, 1000, 2000, 3000, 4000, and 5000 m). The model has a realistic bottom topography, and the annual cycle is resolved. Monthly mean climatologies of wind stress (Hellerman and Rosenstein 1983) and air temperature (COADS; Woodruff et al. 1987) were

used as forcing fields. For the temperature, a Newtonian type of boundary condition with a constant of 40 W m^{-2} K^{-1} was applied. In an initial spinup run the model was started from homogenous water at rest and integrated for 10 000 years to a steady state. In this run, the salinity of the surface layer was relaxed to the climatological surface salinity (Levitus 1982). The freshwater fluxes required to approach the climatological surface salinity were stored and used as forcing for subsequent runs. In a second step the surface salinity was no longer prescribed but the freshwater fluxes were prescribed for another 4000 years of integration. The field obtained at the end of this integration was used as a starting field for subsequent variability and greenhouse experiments.

In the absence of a coupling to an atmospheric general circulation model (AGCM), these "mixed" boundary conditions for heat and salt may be regarded as a reasonable approximate description of the feedback between ocean and atmosphere. Anomalies of the sea surface temperature (SST) are damped out relatively quickly by the resultant heat fluxes and thus have a relatively short lifetime. [According to Frankignoul and Hasselmann (1977), anomalies of the SST in the North Pacific have a typical lifetime of 6 months.] A similar direct feedback for the surface salinity does not exist. Precipitation, evaporation, and runoff from rivers are almost completely independent of the actual surface salinity. Thus, salinity anomalies have a much longer lifetime than anomalies of the SST. This seems true in nature also; for example, the negative salinity anomaly of the 1970s in the northern North Atlantic could be traced for at least 14 years (Dickson et al. 1988). In fact, it appears there may exist a second steady state of the Atlantic thermohaline circulation. This state was first discovered in an OGCM with this type of boundary condition (Bryan 1986), and has since been found in a coupled atmosphere–ocean general circulation model (Manabe and Stouffer 1988).

3. Natural variability

The data from a 3800-year run described in MM provided estimates of the long-term natural oceanic variability. In this experiment, the OGCM presented above was driven by climatological air temperature and fluxes of momentum and fresh water. A spatially correlated (about 25° latitude and longitude) random freshwater flux was superimposed over all the ocean basins with no correlation from month to month. The amplitude of that white noise, taken to be globally almost uniform, was chosen to be 16 mm mo^{-1}, equivalent to 20% of the globally integrated mean precipitation (Baumgartner and Reichel 1975).

A critical parameter in the resulting estimate of the natural variability is of course the amplitude of forcing. Because a global dataset of the net freshwater flux variability was not available, we can only compare the prescribed variability with data from a 20-year AGCM simulation (Latif et al. 1990; W. König, personal communication) forced with observed SST. The simulated variability of precipitation minus evaporation showed typical values of 15 mm mo^{-1} in polar regions and much stronger variability in the tropics with typical values of 100 mm mo^{-1} and more. We conclude that the applied forcing probably has realistic values in high latitudes, but the low-latitude variability was underestimated.

The oceanic response showed strong irregular oscillations with a typical time scale of slightly more than 300 years (Fig. 1). This variability was represented by a single eigenmode of the oceanic circulation, consisting of a dipole salinity anomaly being advected by the mean thermohaline circulation of the Atlantic, interacting and thus modifying the circulation by the changes in the density field. This eigenmode had the largest amplitude in the Southern Ocean. It leads to a sporadic shutdown of Antarctic Bottom Water formation and a 50% change of the mass transport of the Antarctic Circumpolar Current.

Any contribution to the variability that might occur due to variations in wind forcing (e.g., El Niño), air temperature, and any variability due to atmosphere–ocean feedbacks is missing in our simulations. Additionally, the estimate of the resulting natural variability will certainly depend strongly on the choice of the amplitude of the net freshwater flux noise, especially in the Southern Ocean. Our estimate may also depend on the assumed spatial homogeneity of the amplitude of the white noise forcing. Other climatic important

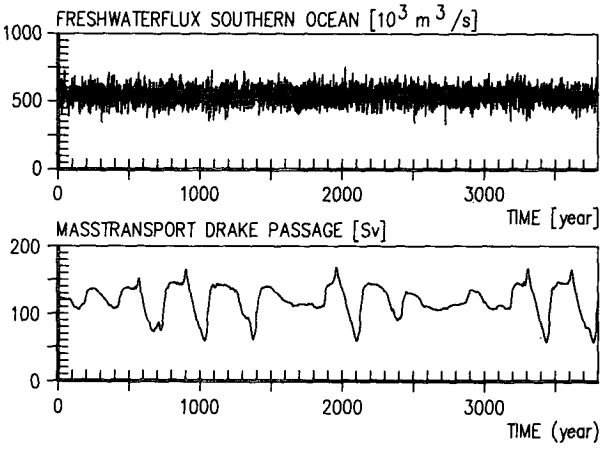

FIG. 1. Time series of the prescribed stochastic net freshwater flux into the Southern Ocean (south of 30°S) and response of the ocean circulation to that forcing. Shown here is the mass transport of the Antarctic Circumpolar Current. The strong irregular oscillations with a typical time scale of slightly more than 300 years are due to the occurrence of a salt oscillator being advected by the mean thermohaline circulation of the Atlantic leading to a sporadic shutdown of bottom water formation in the Southern Ocean and thus reduced mass transport of the Antarctic Circumpolar Current. For details of the experiment see Mikolajewicz and Maier-Reimer (1990).

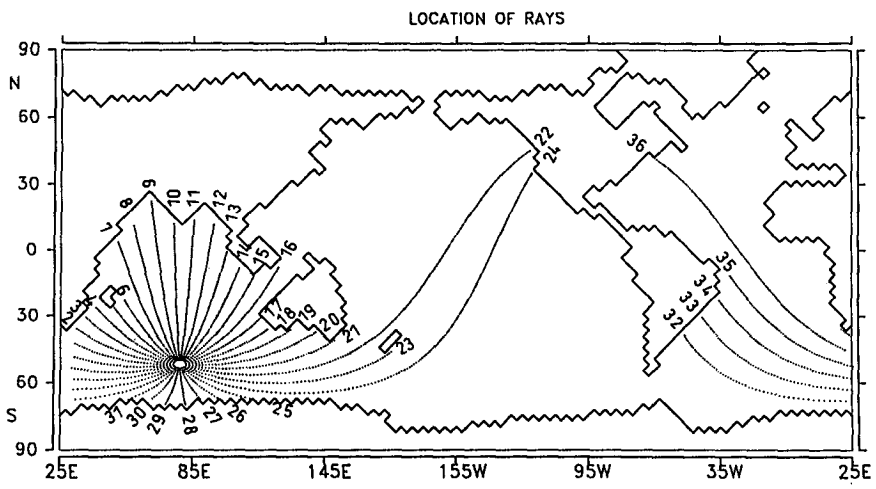

FIG. 2. Location of the acoustic ray paths used in this paper.

processes like changes in the solar irradiance and volcanic eruptions are not included in this model.

Thus, there are large uncertainties connected with these simulations of the natural variability. Consequently, our estimates of the signal-to-noise ratios used in the following sections should be taken as order of magnitude rather than as precise values.

4. Greenhouse signal

Though it is possible to derive the transient oceanic response to increased GHG concentrations from simulations with a coupled ocean–atmosphere general circulation model (e.g., Stouffer et al. 1989; Cubasch et al. 1992; Manabe et al. 1991), we decided to derive the GHG signal in a way that is consistent with the derivation of the estimate of the natural variability. The experiment used here is very similar to the one described by Mikolajewicz et al. (1990, henceforth MSM).

The OGCM was forced by both climatology and monthly mean air temperature anomalies that prescribe the atmospheric response to the greenhouse effect. The anomalous spatial warming pattern was derived from the mean of four experiments with different atmospheric general circulation models, coupled to pure mixed-layer ocean models, for steady-state responses to doubling of atmospheric carbon dioxide concentrations (Geophysical Fluid Dynamics Laboratory: Wetherald and Manabe 1986; Goddard Institute for Space Studies: Hansen et al. 1984; Oregon State University: Schlesinger and Zhao 1989; U.K. Meteorological Office: Wilson and Mitchell 1987). The pattern of change was similar in all experiments, with largest temperature increases near the poles due to the ice–albedo effect, and variations in amplitude only. The global average warming over ocean points from these models was 4 K. We assumed that the spatial structure of the warming was time invariant during the process of the doubling of the carbon dioxide concentrations, and this gave us the spatial pattern of temperature change, $g(x)$. The time dependence of the warming was prescribed by the following function for the amplitude of this pattern: $f(t) = 1 - \exp(t/\alpha)$, with the constant α assumed to be 80 years, this being the only difference between the current work and the experiment of MSM (they used a time constant of 40 years instead). This is equivalent to a global warming of 2.9 K within 100 years.[1] The space–time pattern of GHG-induced change over the oceans was defined to be $\Delta T(x, t) = f(t)g(x)$.

The neglect of atmospheric feedback, anomalous wind stress and freshwater flux forcing, and the assumption of time-invariant patterns of the surface temperature change clearly represent major idealizations of this experiment. Further discussion of the limits of this approach and the changes in ocean circulation as a response to this perturbation is given in MSM.

5. Computation of acoustic travel times

The data were available as averages over two years for both the simulation forced by stochastic moisture flux and the simulation forced by the approximated greenhouse gas warming. For each of these data the three-dimensional sound speed field was computed, and the depth of the minimum of sound speed was determined. The propagation in this sound channel was assumed to be adiabatic (no mode to mode interaction), and only the axial mode was considered. (In the real experiment it might be possible to gain some

[1] This value corresponds the global mean warming Cubasch et al. (1992) found in an experiment with a coupled ocean–atmosphere general circulation model with prescribed GHG concentrations according to the "business as usual" scenario A presented recently in a report from the Intergovernmental Panel of Climate Change (Houghton et al. 1990).

information about the vertical structure of the temporal variations from higher acoustic modes.) Acoustic travel times were computed along 36 paths, which describe the sound propagation from Heard Island in the southern Indian Ocean at angular increments of 10 degrees. The location of the paths is shown in Fig. 2. For simplicity it was assumed that the paths follow the great circles instead of the refracted geodesics. It should not make any significant difference whether one uses great circles or geodesics, as the spatial scales of the variability are much larger than the error induced by this simplification. Temporal changes of the path through changes in the refracted paths are—according to Munk and Wunsch (1987)—a second-order effect. This assumption—including the problem of possible horizontal multipathing—needs to be rigorously tested, a task well outside the scope of the present effort.

6. Estimation of the S/N ratio for a single path

For a detailed analysis of the signal-to-noise ratio for the changes in travel time along a single path, we choose the longest of the main paths proposed by MF from Heard Island to Coos Bay (number 22 in Fig. 2). This path has to cross the relatively shallow Tasman Sea, where the depth of the sound speed minimum partly reaches the bottom. In the feasibility experiment in January 1991, however, the signals were weaker than the Atlantic arrivals, but not too weak to prevent an analysis (W. Munk, personal communication). Within the limitations of our approach, as mentioned above, we have included it to demonstrate our methodology.

The time series of changes in travel time due to the natural variability, as determined from the stochastic moisture flux simulation, was divided into overlapping intervals of 10 years length. The trend was determined by linear regression for each of these intervals. The resulting probability distribution for the change in travel time is shown in Fig. 3a. Years 10–50 of the greenhouse warming experiment were used to derive an average signal, yielding an expected change in travel time of -0.39 s yr^{-1}. The changes in the travel times in the greenhouse experiment were almost constant in this period. As can be seen from Fig. 3a, there is a good chance (20%) that a change of this magnitude or greater in acoustic travel time can be obtained by natural variability alone.

The same procedure as above was repeated, but now with an interval length of 20 years (Fig. 3b). In this case the probability of obtaining the expected change in acoustic travel time by natural variability alone is substantially reduced to about 6%.

We next investigated whether there are other paths for which the S/N ratio might be more favorable. First, we computed the horizontal distribution of the standard deviation of the sound speed on the actual depth of the sound speed minimum, shown in Fig. 4a. The field shows by far the largest amplitudes in the Southern

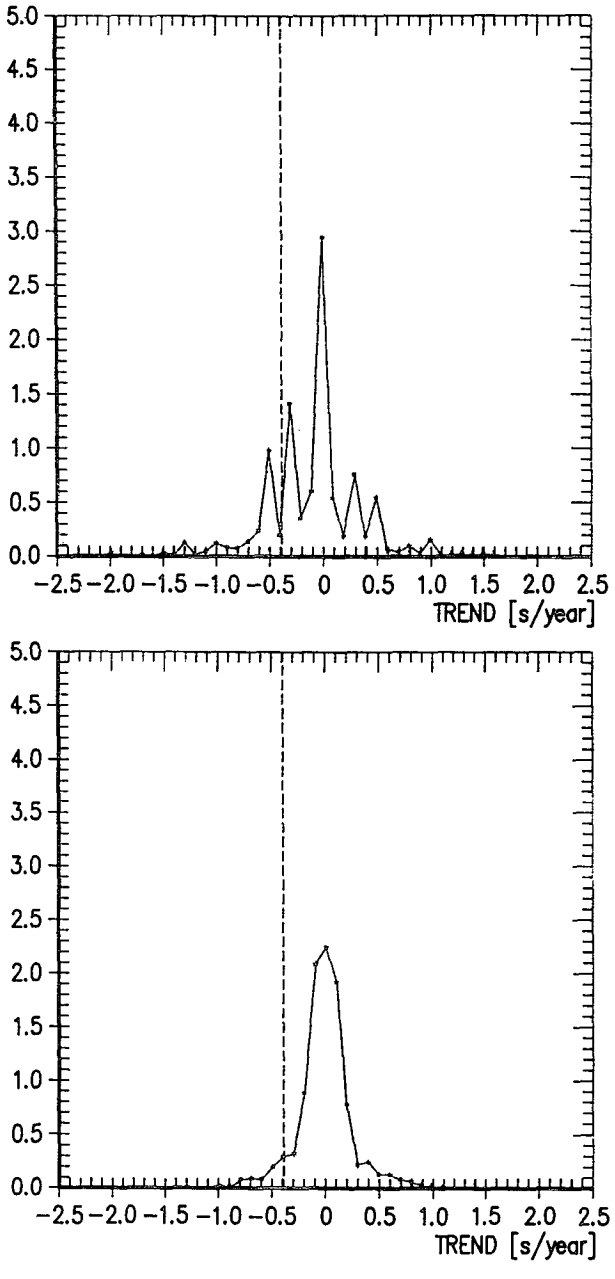

FIG. 3. (a) Probability distribution of the trends on 10-year-long intervals of the stochastically forced experiment for the sound transmission from Heard Island to Coos Bay (No. 22 in Fig. 2). The stippled line shows the signal obtained from the greenhouse experiment. The area to the left of this value corresponds to 20%. (b) As (a) but with interval length of 20 years. The area to the left of the stippled line corresponds to a total probability of 6%.

Ocean, with extreme values higher than 10 m s^{-1}, but there are significant noise levels in the northern Atlantic and Pacific as well. In low and middle latitudes the variability is about one order of magnitude lower, with typical values around 1 m s^{-1}. Simulations of El Niño events with a similar model (Barnett et al. 1991) in-

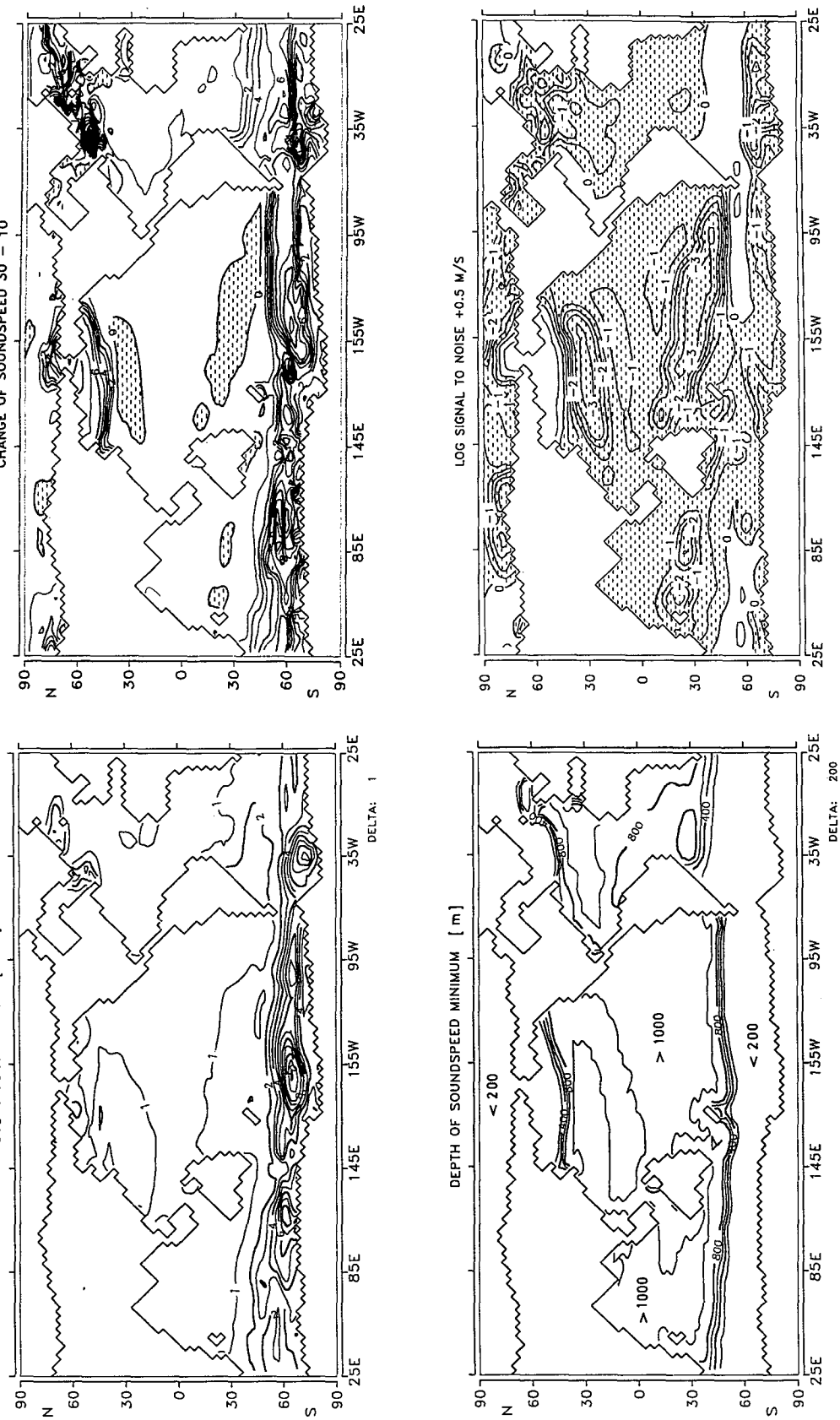

FIG. 4. (a) Horizontal distribution of the standard deviation of the sound speed in the actual minimum of the sound speed from the stochastically forced experiment. Values are given in meters per second. (b) Horizontal distribution of the change in sound speed in the respective minimum between years 10 and 30 of the greenhouse experiment. Values are given in meters per second, stippled areas correspond to negative values. (c) Average depth of the sound speed minimum during the 3800 years of the stochastically forced experiments. (d) Horizontal distribution of the logarithm of the ratio between signal (change in sound speed between years 10 and 30 of greenhouse experiment) and the standard deviation of the noise. To attribute for the contribution from eddies and measurement errors, a constant value of 0.5 m s^{-1} has been added to the noise. Stippled areas correspond to regions, where the greenhouse signal does not exceed one standard deviation of the natural variability.

dicated an amplitude of interannual temperature fluctuations in the tropical Pacific in the order of 0.1 K, which corresponds to 0.4 m s^{-1} in sound speed (Latif, personal communication).

This pattern from the stochastically forced run was compared with the computed changes in the sound speed minimum between years 10 and 30 of the greenhouse warming experiment (Fig. 4b). It becomes obvious that the expected signal is strongest where the amplitudes of the natural variability are also strongest, especially in the Southern Ocean.

For the computation of the S/N ratio (Fig. 4d), a spatially constant contribution of 0.5 m s^{-1} from eddies and measurement errors were included. This value corresponds to the mean value for the mesoscale eddies given by Semtner and Chervin (1990).

Except for the western Atlantic, the S/N ratio of changes of sound speed at low latitudes is generally unfavorable for detection studies, which can be entirely explained by the weakness of the signal. The time for the signal to reach the water masses at 1000-m depth has simply been too short to allow a strong signal to develop. In the northern oceans the S/N ratio seems to be more favorable. But many of these regions cannot be reached by the rays from Heard Island. Although the natural variability has its maxima in the Southern Ocean, the results show that the S/N ratio in this region is still favorable for detection studies.

Both signal and noise show largest amplitudes where the depth of the sound speed minimum is shallower than 200 m (Fig. 4c). Thus, the signals measured with the array proposed will not—as originally estimated by MF—be a good measure of the temperature changes in middle and low latitudes at depths around 1000 m, but rather an indicator of changes in the near-surface waters of the Southern Ocean. For example, the path between Heard Island and Coos Bay will receive about two-thirds of its natural variability from the first one-third of its path in the Southern Ocean. The greenhouse signal comes almost entirely (95%) from the first one-third of the path. To obtain the signals from extrapolar regions, additional receivers would be required at locations that allow the elimination of the polar contribution to the overall changes in travel time.

A real array would not be restricted to the sound axis but would gain additional information about the vertical structure from different modes and thus sample the signals at low latitudes and shallow depths, where the greenhouse signal is considerably stronger than at the sound axis. In this first study, we have ignored this potentially important additional information.

7. Estimation of the S/N ratio for an ensemble of paths

One of the main problems for pattern detection is the large number of degrees of freedom in space. Thus, the number of degrees of freedom has to be reduced drastically for application. In this paper, two different methods of deriving a detection pattern with optimal S/N characteristics are applied.

The first approach to estimating an optimal detection pattern was derived from the dominant patterns of natural variability. In order to estimate the magnitude of the probability of detecting the greenhouse effect with an array of receivers with a source on Heard Island, the information from all 36 paths shown in Fig. 2 was used. Since large spatial scales characterize both signal and natural variability, it must be expected that records from adjacent receivers will show a similar temporal behavior. In order to extract the most important patterns of temporal change, an EOF analysis was performed on the time series of the trends obtained from the natural variability experiment at each of the 36 receivers (Fig. 2). Applied on the intervals of 10 years length, the first EOF explained 40.7% and the second 16.9% of the variance. In the case of the 20-year interval, the respective numbers are 46.9% and 21.9%. In both cases, the first two EOFs explained about 60% of the natural variability. Thus, it is reasonable to assume that the basic behavior of the natural variability (noise) can be approximated by these two patterns alone.

The distribution of the almost 1900 pairs of the principal component (PC) time series for pattern of changes in acoustic travel time is shown in Fig. 5. Each pair of PCs was obtained from the trend of one 10-year interval of record from the stochastically forced experiment. Also shown is the projection of the expected signal on these two noise EOFs. The most favorable situation for detectability would be for the signal to be clearly outside the swarm covered by the different realizations of the natural variability. In the case of the 10-year intervals (Fig. 5a), the signal is still well within the space covered by the noise. For longer intervals (see Fig. 5b), the situation becomes more favorable, the signal being on the outer edge of the noise distribution.

The linear combination (rotation) optimal for detection between the two EOFs turned out to be a direction of 60 degrees relative to the first EOF (Fig. 5b). The distribution of the time coefficients of the first two EOFs projected on this line is shown in Fig. 6. For an interval length of 10 years there is a probability of 7% of obtaining the expected greenhouse signal by natural variability alone, whereas for an interval length of 20 years this probability is reduced to 3%. The increase in probability of detection obtained by using more receivers, and thus higher spatial resolution as compared to the analysis of one path only, is obvious and not surprising. Thus, the use of multiple receivers should overcome the disappointing results mentioned earlier. It might be possible to increase the detection probability further by the use of additional receivers located in island stations in the interior of the oceans, thereby allowing extraction of the signal also from extrapolar regions, as intended by MF.

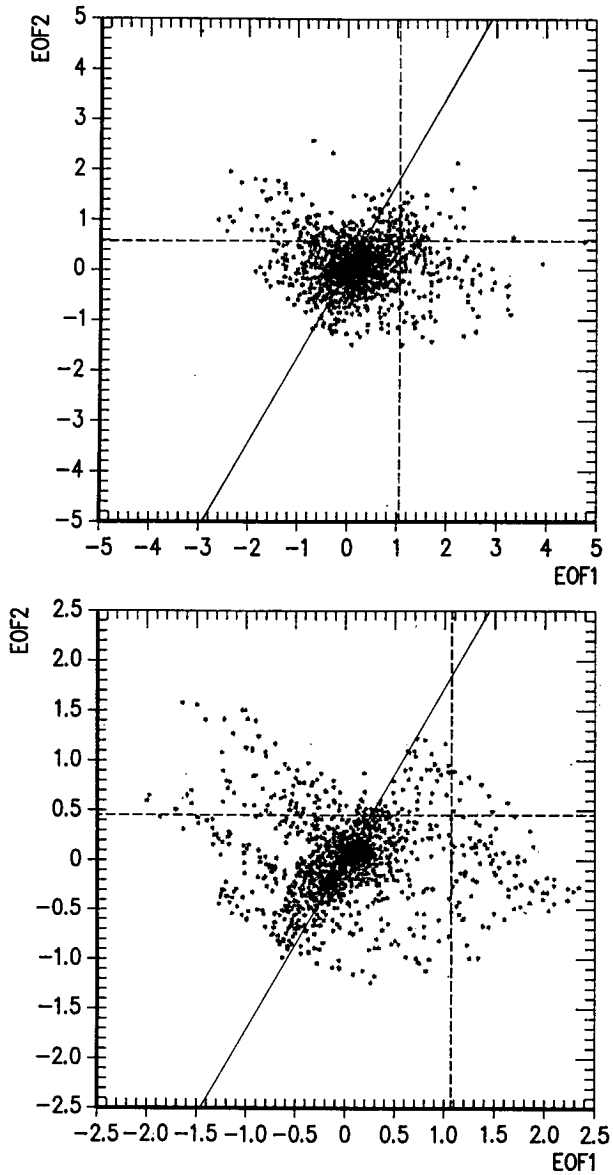

FIG. 5. (a) Scatterplot of the principal components of the first two noise EOFs from all 36 receiver time series for a record length of 10 years. The projection of the expected greenhouse signal onto these two EOFs is indicated by the dashed lines. (b) As in (a) but for a record length 20 years. The solid line indicates the position of the optimal detection pattern (60° relative to EOF1).

The loadings for the different stations for the first two noise EOFs, the linear combination of them that is optimal for detection, and the normalized signal are given in Table 1 for the case of the 20-year record length. It can be seen that for the optimal detection pattern the two EOFs were combined in a way that they eliminated the contribution from the path from Heard Island to San Francisco (number 24 in Fig. 2). In contrast, the path to the east coast of the United States (number 36) gained a higher weight, being the path with the highest loading in the combined pattern. One could follow this line of thought and design a truly optimal array of receivers to minimize both cost and number of sites while maximizing detection probability. Clearly, 36 receivers is far more than needed for the task.

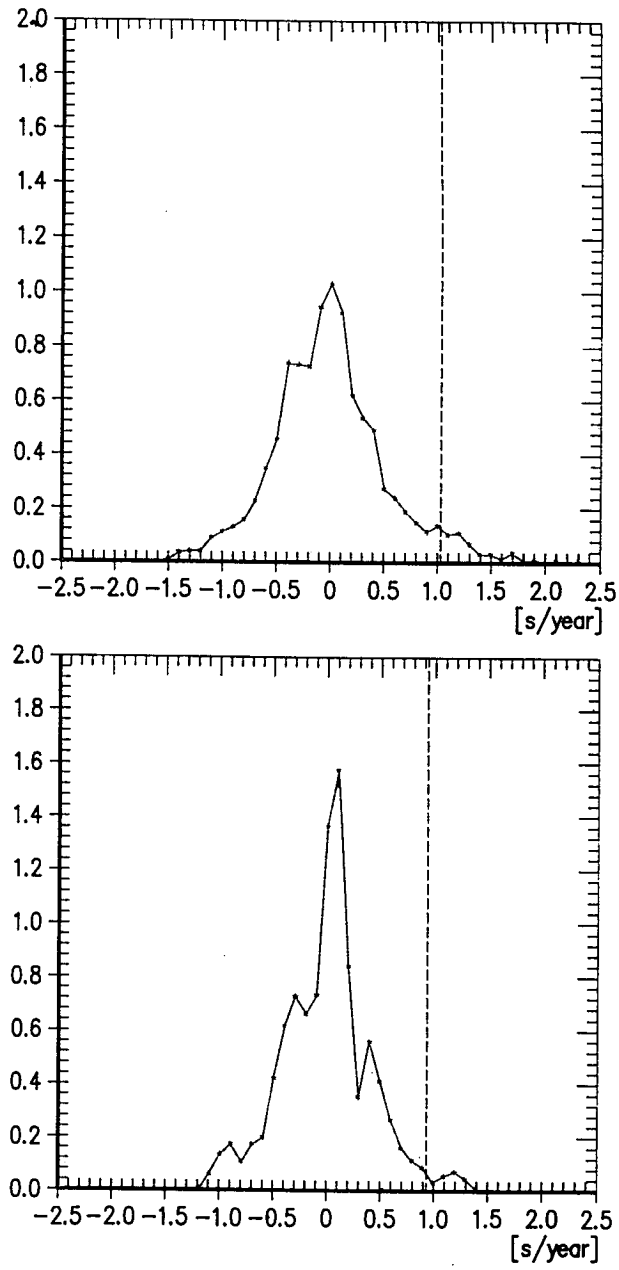

FIG. 6. (a) Probability distribution of the projection of the trends of the stochastically forced experiment projected onto the optimal detection pattern for a record length of 10 years. The dashed line indicates the projection of the signal from the greenhouse experiment onto the optimal pattern. The area to the right of the dashed line corresponds to a probability of 7%. (b) As in (a) but for a record length of 20 years. The area to the right of the dashed line corresponds to a probability of 3%.

TABLE 1. Loadings of the noise EOFs, the optimal detection pattern, and the normalized greenhouse signal, all for 20-year intervals. For location of the paths see Fig. 2.

Number	EOF1	EOF2	Optimal pattern	Normal signal
1	−0.018	−0.257	−0.232	−0.136
2	0.003	−0.274	−0.236	−0.098
3	0.003	−0.258	−0.222	−0.063
4	−0.009	−0.216	−0.191	−0.045
5	−0.019	−0.180	−0.166	−0.037
6	−0.026	−0.156	−0.148	−0.031
7	−0.055	−0.166	−0.171	−0.027
8	−0.061	−0.166	−0.174	−0.028
9	−0.077	−0.182	−0.196	−0.030
10	−0.062	−0.161	−0.170	−0.029
11	−0.069	−0.167	−0.179	−0.029
12	−0.069	−0.165	−0.177	−0.030
13	−0.066	−0.151	−0.164	−0.033
14	−0.065	−0.143	−0.157	−0.038
15	−0.072	−0.143	−0.160	−0.045
16	−0.087	−0.152	−0.175	−0.053
17	−0.086	−0.115	−0.143	−0.054
18	−0.109	−0.094	−0.136	−0.058
19	−0.157	−0.050	−0.122	−0.066
20	−0.202	0.004	−0.098	−0.112
21	−0.230	0.007	−0.054	−0.210
22	−0.425	0.008	−0.143	−0.293
23	−0.437	0.236	−0.014	−0.242
24	−0.510	0.301	0.005	−0.292
25	−0.165	0.032	−0.054	−0.153
26	−0.137	0.005	−0.064	−0.140
27	−0.119	−0.031	−0.087	−0.113
28	−0.107	−0.062	−0.107	−0.119
29	−0.085	−0.078	−0.110	−0.100
30	−0.063	−0.084	−0.105	−0.094
31	−0.054	−0.093	−0.108	−0.103
32	−0.134	−0.239	−0.274	−0.301
33	−0.198	−0.193	−0.266	−0.368
34	−0.144	−0.152	−0.203	−0.390
35	−0.072	−0.153	−0.169	−0.310
36	−0.118	−0.287	−0.308	−0.284

The similarity between the patterns of natural variability and greenhouse signal can be expressed by dot products (pattern correlations) between the noise EOFs and the normalized pattern of the expected signal (Cubasch et al. 1991). The first noise EOF describes a pattern relatively similar to the expected signal (0.81). But the second noise EOF pattern strongly differs from the signal, since the associated dot product is only 0.35. The pattern of optimal detectability, the rotated EOF, reaches a value of 0.71 when compared with the expected signal. This again suggests that reduction of the total number of receivers might be possible without significantly decreasing the probability of detection.

For instance, one could increase the detectability of the signal further by assigning different weights for single receivers; for example, in this case rule out the San Francisco path and put a higher weight on the path to the U.S. East Coast. However, the point would very rapidly be reached where information about small scales would dominate (e.g., by subtraction of adjacent paths, etc.). This information is certainly not reliable in the numerical simulations used here. Furthermore, the original idea of using large-scale patterns in the detection strategy would be lost.

The preceding considerations do not exclude the possibility that a major component of the signal is not contained in the noise and thus will not contribute to the signal-to-noise ratio when the signal is projected onto the major components of the natural variability.

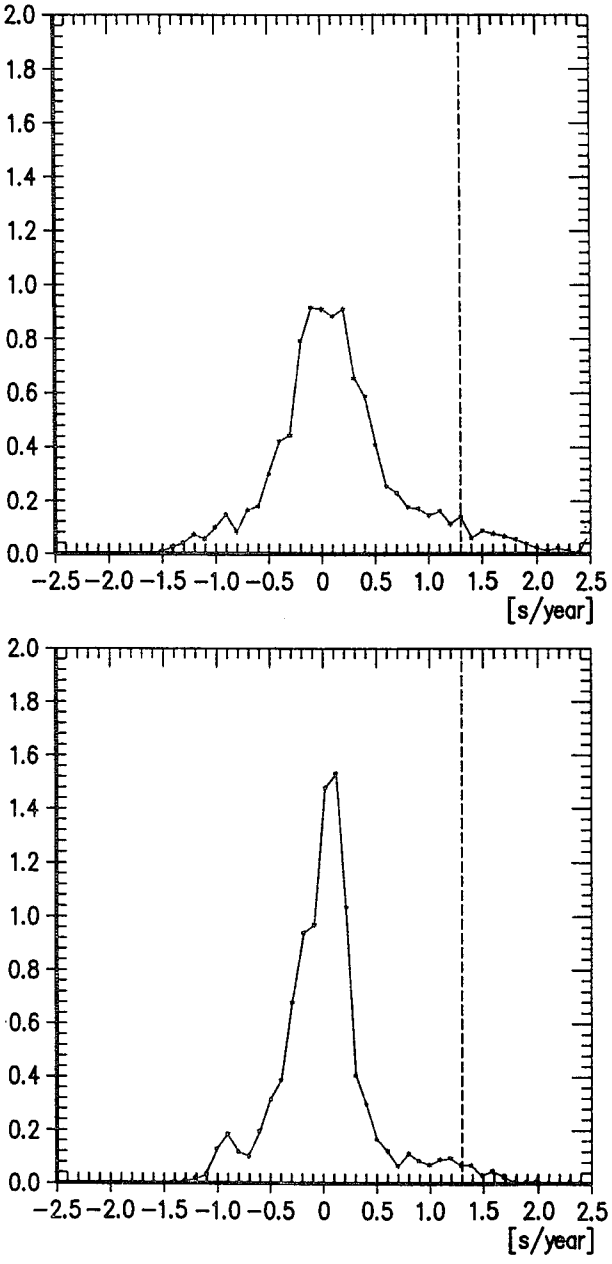

FIG. 7. Probability distribution of the stochastically forced experiment projected onto the normalized greenhouse signal for interval lengths (a) of 10 and (b) of 20 years. The dashed line indicates the strength of the greenhouse signal. The area to the right of the dashed line corresponds to probabilities of 6% and 3%, respectively.

To investigate this, the dot product between the normalized pattern of change of the signal and every single realization of the natural variability was computed, thus effectively projecting the noise onto the signal. The distribution of the resulting values for the dot products is shown in Fig. 7. At least in the case of the 20-year record lengths the signal is well off the main noise region, yielding a probability of about 3% of obtaining the expected greenhouse-induced pattern by natural variability alone. In the case of the 10-year intervals this probability is 6%. These are almost identical to the probabilities found above. For detectability, it does not seem to make a significant difference whether one projects the noise on the expected signal or whether one projects the signal on the major components of the noise. These results confirm our earlier approach to estimating the detection uncertainties.

8. Conclusions

The main objective of this paper was to demonstrate how one might approach the problem of estimating the ratio of the greenhouse signal to natural variability (noise) on a decadal time scale. Certainly there are large uncertainties associated with the strongly simplified estimates of both signal and noise presented here. Nevertheless, we conclude that there is a realistic chance of detecting the expected greenhouse gas–induced warming in the World Ocean by changes in travel times of long-range acoustic rays. This approach to greenhouse signal detection thereby gives a valuable additional indication of climatic change, and will—when used together with information from other existing measurements—increase the probability of detecting the greenhouse effect.

The measured changes in acoustic travel time from a source near Heard Island will be dominated by processes in the noisy near-surface layers of the south Indian and South Atlantic oceans. By appropriate positioning of additional receivers it might be possible to extract the signals from middepths at lower latitudes as well, but they will likely be approximately one order of magnitude smaller than those from the Southern Ocean. Our study also suggests that detection probability would presumably be increased by placing the—or an additional—acoustic source outside the zone of strong polar variability.

Acknowledgments. We appreciated discussion with Walter Munk and Klaus Hasselmann. Ben Santer and Hans von Storch read a first draft of this paper and made valuable suggestions. Thanks are also to two anonymous reviewers. Tony Tubbs performed the EOF analysis and helped with plot routines. We also thank Marion Grunert and Heinke Höck for work on the illustrations. Support was provided for one of us (TPB) through the Climate Division Program of the National Science Foundation through Grant ATM88-14571 and the Scripps Institution of Oceanography.

REFERENCES

Barnett, T. P., 1983: Long-term changes in dynamic height. *J. Geophys. Res.*, **88**(C14), 9547–9552.

——, 1986: Detection of changes in the global troposphere temperature field induced by greenhouse gases. *J. Geophys. Res.*, **91**(D6), 6659–6667.

——, 1991: An attempt to detect the greenhouse gas signal in a transient GCM simulation. *Greenhouse-Gas-Induced Climatic Change: A Critical Appraisal of Simulations and Observations,* M. E. Schlesinger, Ed., Elsevier, 559–568.

——, and M. E. Schlesinger, 1987: Detecting changes in global climate Induced by greenhouse gases. *J. Geophys. Res.*, **92**(D12), 14 772–14 780.

——, M. Latif, E. Kirk, and E. Roeckner, 1991: On ENSO physics. *J. Climate,* **4,** 487–515.

Baumgartner, A., and E. Reichel, 1975: Die Weltwasserbilanz. Oldenbourg Verlag, München, 179 pp.

Bryan, F., 1986: High latitude salinity effects and interhemispheric thermohaline circulations. *Nature,* **305,** 301–304.

Cubasch, U., K. Hasselmann, H. Höck, E. Maier-Reimer, U. Mikolajewicz, B. D. Santer, and R. Sausen, 1992: Time-dependent greenhouse warming computations with a coupled ocean–atmosphere model. *Clim. Dyn.,* **8,** 55–69.

Dickson, R. R., J. Meincke, S.-A. Malmberg, and A. J. Lee, 1988: The "Great Salinity Anomaly" in the Northern North Atlantic 1968–1982. *Progress in Oceanography,* Vol 20, Pergamon 103–151.

Frankignoul, C., and K. Hasselmann, 1977: Stochastic climate models. Part II: Application to sea-surface temperature anomalies and thermocline variability. *Tellus,* **29,** 289–305.

Hansen, J., A. Lacis, D. Rind, G. Russell, P. Stone, I. Fung, R. Ruedy, and J. Lerner, 1984: Climate sensitivity: Analysis of feedback mechanisms. *Climate Processes and Climate Sensitivity,* J. Hansen and T. Takahashi, Eds. Amer. Geophys. Union, 130–163.

Hasselmann, K., 1976: Stochastic climate models. Part I: Theory. *Tellus,* **28,** 473–485.

——, 1982: An ocean model for climate variability studies. *Prog. Oceanogr.,* **11,** 69–92.

Hellermann, S., and M. Rosenstein, 1983: Normal monthly wind stress data over the world ocean with error estimates. *J. Phys. Oceanogr.,* **13,** 1093–1104.

Houghton, J. T., G. J. Jenkins, and J. J. Ephraims, 1990: Climate Change. The IPCC Scientific Assessment. Cambridge University Press, 364 pp.

Latif, M., E. Maier-Reimer, and D. J. Olbers, 1985: Climate variability studies with a primitive equation model of the Equatorial Pacific. *Coupled Ocean–Atmosphere Models,* J. C. J. Nihoul, Ed., Elsevier, 63–81.

——, J. Biercamp, H. von Storch, M. J. McPhaden, and E. Kirk, 1990: Simulation of ENSO-related surface wind anomalies with an atmospheric GCM forced by observed SST. *J. Climate,* **3,** 509–521.

Lemke, P., 1977: Stochastic climate models. Part 3: application to zonally averaged energy models. *Tellus,* **29,** 385–392.

Levitus, S., 1982: Climatological Atlas of the World Ocean. NOAA Prof. Paper 13, Rockville, MD.

Maier-Reimer, E., U. Mikolajewicz, and K. Hasselmann, 1993: Mean circulation of the Hamburg LSG OGCM and its sensitivity to the thermohaline surface forcing. *J. Phys. Oceanogr.,* **23,** 731–757.

Manabe, S., and R. J. Stouffer, 1989: Two stable equilibria of a coupled ocean–atmosphere model. *J. Climate,* **1,** 841–866.

——, ——, M. J. Spelman, and K. Bryan, 1991: Transient responses of a coupled ocean–atmosphere model to gradual changes of atmospheric CO_2. Part I: Annual mean response. *J. Climate,* **4,** 785–818.

Mikolajewicz, U., and E. Maier-Reimer, 1990: Internal secular variability in an OGCM. *Clim. Dyn.,* **4,** 145–156.

——, B. D. Santer, and E. Maier-Reimer, 1990: Ocean response to greenhouse warming. *Nature,* **345,** 589–593.

Munk, W., and C. Wunsch, 1987: Bias in acoustic travel time through an ocean with adiabatic range-dependence. *Geophys. Astrophys. Dyn.*, **39**, 1–24.

——, and A. M. G. Forbes, 1989: Global ocean warming: An acoustic measure? *J. Phys. Oceanogr.*, **19**, 1765–1778.

Reynolds, R. W., 1979: A stochastic forcing model of sea surface temperature anomalies in the North Pacific and North Atlantic. Climatic Research Institute, Report No. 8, Oregon State University, 23 pp.

Santer, B. D., T. M. L. Wigley, P. D. Jones, and M. E. Schlesinger, 1991: Multivariate methods for the detection of greenhouse-gas-induced climate change. *Greenhouse-Gas-Induced Climatic Change: A Critical Appraisal of Simulations and Observations*, M. E. Schlesinger, Elsevier, 511–536.

Schlesinger, M. E., and Z.-C. Zhao, 1989: Seasonal climate changes induced by doubled CO_2 as simulated by the OSU atmospheric GCM mixed-layer ocean model. *J. Climate*, **2**, 459–495.

Semtner, A. J., and R. M. Chervin, 1990: Environmental effects on acoustic measures of global ocean warming. *J. Geophys. Res.*, **95**(C8), 12 973–12 982.

Spiesberger, J. L., and K. Metzger, 1991: Basin-scale tomography: A new tool for studying weather and climate. *J. Geophys. Res.*, **96**, 4869–4889.

——, T. G. Birdsall, and K. Metzger, 1983: Acoustic thermometer. Office of Naval Research Contract N00014-82-C-0019.

Stouffer, R. J., S. Manabe, and K. Bryan, 1989: Interhemispheric asymmetry in climate response to a gradual increase of atmospheric CO_2. *Nature*, **342**, 660–662.

Wetherald, R. T., and S. Manabe, 1986: An investigation of cloud cover change in response to thermal forcing. *Clim. Change*, **8**, 5–23.

Wigley, T. M. L., and S. C. B. Raper, 1990: Natural variability of the climate system and detection of the greenhouse effect. *Nature*, **344**, 324–327.

Wilson, C. A., and J. F. B. Mitchell, 1987: A doubled CO_2 climate sensitivity experiment with a global climate model including a simple ocean. *J. Geophys. Res.*, **92**, 13 315–13 343.

Woodruff, S. D., R. J. Slutz, R. L. Jenne, and P. M. Steurer, 1987: A comprehensive ocean–atmosphere data set. *Bull. Amer. Meteor. Soc.*, **68**, 1239–1250.